OPEN ACCESS Freely available online

PLOS ONE

Numerical Study of Boundary Layer Flow and Heat Transfer of Oldroyd-B Nanofluid towards a Stretching Sheet

Sohail Nadeem[1], Rizwan Ul Haq[1]*, Noreen Sher Akbar[2], Changhoon Lee[3], Zafar Hayat Khan[4]

1 Department of Mathematics, Quaid-I-Azam University, Islamabad, Pakistan, **2** DBS&H, National University of Science and Technology, Islamabad, Pakistan, **3** Department of Computational Science and Engineering, Yonsei University, Seoul, South Korea, **4** School of Mathematical Sciences, Peking University, Beijing, P.R. China

Abstract

In the present article, we considered two-dimensional steady incompressible Oldroyd-B nanofluid flow past a stretching sheet. Using appropriate similarity variables, the partial differential equations are transformed to ordinary (similarity) equations, which are then solved numerically. The effects of various parameters, namely, Deborah numbers β_1 and β_2, Prandtl parameter Pr, Brownian motion N_b, thermophoresis parameter N_t and Lewis number L_e, on flow and heat transfer are investigated. To see the validity of the present results, we have made the comparison of present results with the existing literature.

Citation: Nadeem S, Ul Haq R, Akbar NS, Lee C, Khan ZH (2013) Numerical Study of Boundary Layer Flow and Heat Transfer of Oldroyd-B Nanofluid towards a Stretching Sheet. PLoS ONE 8(8): e69811. doi:10.1371/journal.pone.0069811

Editor: Nikolai Lebedev, US Naval Reseach Laboratory, United States of America

Received March 2, 2013; **Accepted** June 12, 2013; **Published** August 27, 2013

Funding: This work was supported by a National Research Foundation of Korea grant funded by the Korea government (2010-0023303, R31-2008-000-10049-0, 201331022.01). The funders had no role in study design, data collection and analysis, decision to publish, or preparation of the manuscript.

Competing Interests: The authors have declared that no competing interests exist.

* E-mail: ideal_riz@hotmail.com

Introduction

The flow over a stretching sheet has been premeditated because of its numerous industrial applications such as industrialized of polymer sheet, filaments and wires. Through the mechanized process, the stirring sheet is assumed to extend on its own plane and the protracted surface interacts with ambient fluid both impulsively and thermally. Only Navier Stokes equations are deficient to explain the rheological properties of fluids. Therefore, rheological non-Newtonian fluid models have been proposed to overcome this deficiency. Sakiadis [1] was the first who discussed the boundary layer flow over a stretching surface. He discussed numerical solutions of laminar boundary-layer behavior on a moving continuous flat surface. Experimental and analytical behavior of this problem was presented by Tsou et al. [2] to show that such a flow is physically possible by validating Sakiadis [1] work. Crane [3] extended the work of Sakiadis [1] for both linear and exponentially stretching sheet considering steady two-dimensional viscous flow. Free convection on a vertical stretching surface was discussed by Wang [4]. Heat transfer analysis over an exponentially stretching continuous surface with suction was presented by Elbashbeshy [5]. He obtained similarity solutions for the laminar boundary layer equations describing heat and flow in a quiescent fluid driven by an exponentially stretching surface subject to suction. Viscoelastic MHD flow heat and mass transfer over a stretching sheet with dissipation of energy and stress work was discussed by Khan et al. [6]. Ishak et al. [7] studied heat transfer over a stretching surface with variable heat flux in micropolar fluids. Nadeem et al. [8] coated boundary layer flow of a Jeffrey fluid over an exponentially stretching surface with radiation effects. Recently in another article Nadeem et al. [9] investigated the magnetohydrodynamic (MHD) boundary layer flow of a Casson fluid over an exponentially permeable shrinking sheet.

The term ''Nanofluids'' is used for the fluids having suspension of nano-sized metallic or non-metallic particles. The main idea of using nanoparticles is to enhance the thermal properties of a base fluid. Invokement of nanofluids with improved heat distinctiveness can be noteworthy in stipulations of more competent cooling systems, consequential in higher productivity and energy savings. Several prospective applications for nanofluids are heat exchangers, radiators for engines, process cooling systems, microelectronics, etc. Choi [10] was the first who have made the analysis on nanoparticles in 1995. Xuan and Roetzel [11] presented cautiously the flow of a nanofluid in a tube using a dispersal replica. Heat transfer enhancement in a two-dimensional flow utilizing nanofluids is presented by Khanafer et al. [12]. They discussed the problem physically for various flow parameters. The Cheng–Minkowycz problem of natural convection past a vertical plate, in a porous medium saturated by a nanofluid is studied analytically by Nield and Kuznetsov [13]. The use of nanofluid model incorporates the effects of Brownian motion and thermophoresis parameter. The natural convective boundary layer flow of a nanofluid over a vertical plate is studied analytically by Kuznetsov and Nield [14]. They found that the reduced Nusselt number is a decreasing function of thermophoresis number and Brownian motion number. The boundary-layer flow and heat transfer in a viscous fluid containing metallic nanoparticles over a nonlinear stretching sheet are analyzed by Hamad and Ferdows [15]. They studied different types of nanoparticles and found that the behavior of the fluid flow changes with the change of the

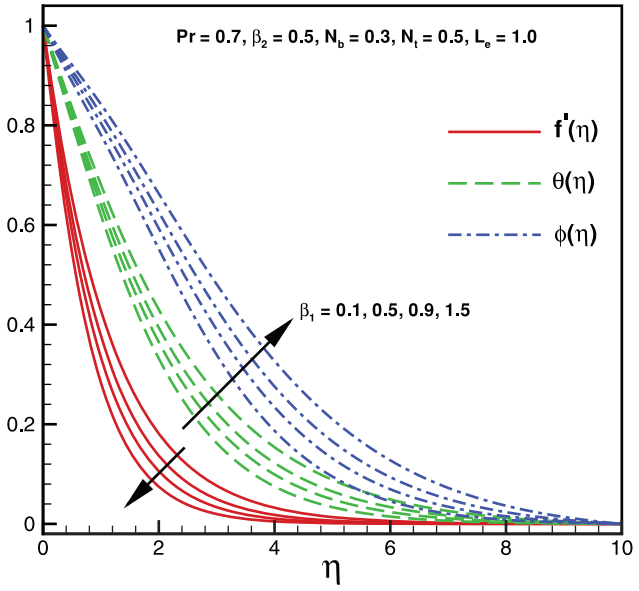

Figure 1. Variation of velocity, temperature and nanoparticles fraction for various values of β_1.
doi:10.1371/journal.pone.0069811.g001

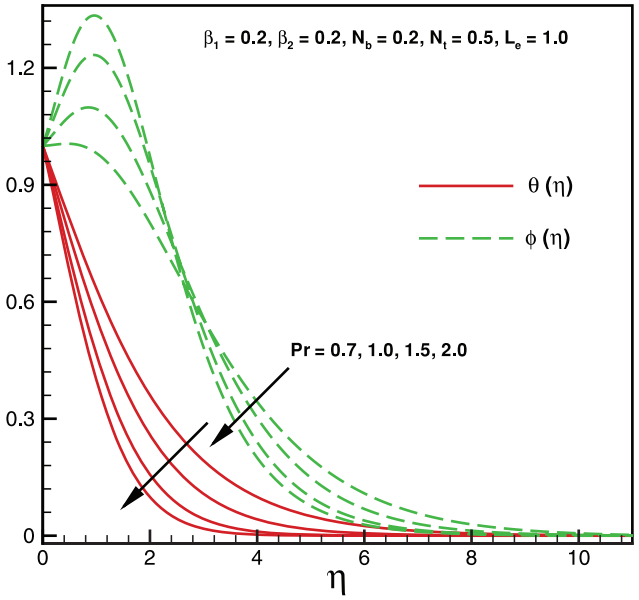

Figure 3. Variation of temperature and nanoparticles fraction for various values of Pr.
doi:10.1371/journal.pone.0069811.g003

nanoparticles type. Numerous recent studies on nanofluids can be found in Refs. [16–25].

Main objective of the present article is to discuss the Oldroyd B nanofluid flow model over a stretching sheet. Mathematical model of the proposed study has been constructed after applying the boundary layer approach. Then, invoking the similarity transformation, we reduce the system of nonlinear partial differential equations into the system of nonlinear ordinary differential equations. The reduced couple nonlinear ODEs are solved numerically. Excellent comparison of the present approach has presented with the previous literature. The effects of various flow controlling parameters on the velocity, temperature and mass fraction function profiles are discussed. Moreover, variation of the local Nusselt and Sherwood number for various nanoparticles parameters has been constructed. The formulation of the paper is designed as follow. The problem formulation is presented in section two. The numerical solutions graphically with physical interpretation are incorporated in section three. Section four contains the summary of the whole analysis.

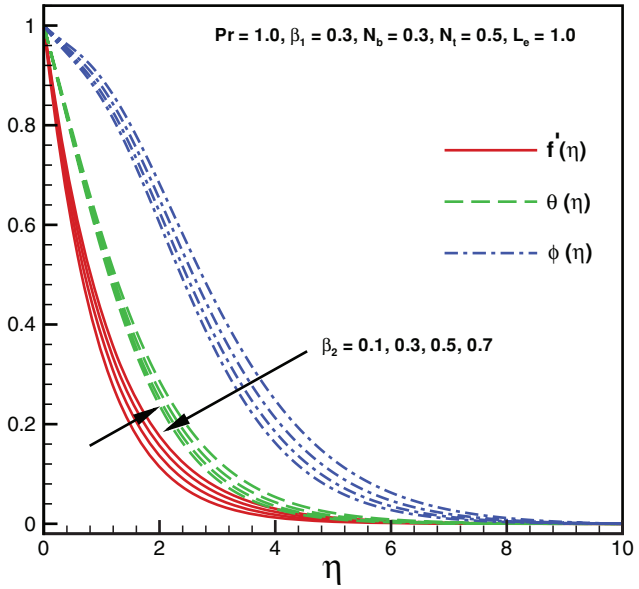

Figure 2. Variation of velocity, temperature and nanoparticles fraction for various values of β_2.
doi:10.1371/journal.pone.0069811.g002

Problem Formulation

Consider two-dimensional steady incompressible Oldroyd-B fluid past a stretching sheet. In addition, nanoparticles effects are saturated, while sheet is stretching along the plane $y=0$. The flow is assumed to be confined to $y>0$. Here we assumed that the sheet is stretched with the linear velocity $u(x)=ax$, where $a>0$ is constant and $x-$axis is measured along the stretching surface. The boundary layer equations of Oldroyd-B fluid model along with the thermal energy and nanoparticles equations for nanofluids are

$$\frac{\partial u}{\partial x}+\frac{\partial v}{\partial y}=0, \tag{1}$$

$$u\frac{\partial u}{\partial x}+v\frac{\partial u}{\partial y}+\Lambda_1(u^2\frac{\partial^2 u}{\partial x^2}+v^2\frac{\partial^2 u}{\partial y^2}+2uv\frac{\partial^2 u}{\partial x\partial y})= v\left\{\frac{\partial^2 u}{\partial y^2}+\Lambda_2(u\frac{\partial^3 u}{\partial x\partial y^2}+v\frac{\partial^3 u}{\partial y^3}-\frac{\partial u}{\partial x}\frac{\partial^2 u}{\partial y^2}-\frac{\partial u}{\partial y}\frac{\partial^2 v}{\partial y^2})\right\}, \tag{2}$$

$$u\frac{\partial T}{\partial x}+v\frac{\partial T}{\partial y}=\alpha(\frac{\partial^2 T}{\partial x^2}+\frac{\partial^2 T}{\partial y^2})+\tau\{D_B(\frac{\partial C}{\partial x}\frac{\partial T}{\partial x}+\frac{\partial C}{\partial y}\frac{\partial T}{\partial y}) +(\frac{D_T}{T_\infty})[(\frac{\partial T}{\partial x})^2+(\frac{\partial T}{\partial y})^2]\}, \tag{3}$$

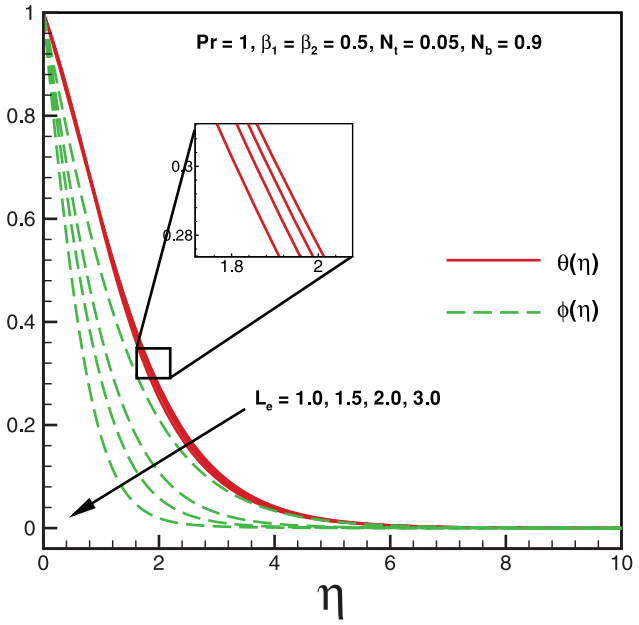

Figure 4. Variation of temperature and nanoparticles fraction for various values of L_e.
doi:10.1371/journal.pone.0069811.g004

$$u\frac{\partial C}{\partial x}+v\frac{\partial C}{\partial y}=D_B\left(\frac{\partial^2 C}{\partial x^2}+\frac{\partial^2 C}{\partial y^2}\right)+\left(\frac{D_T}{T_\infty}\right)\left(\frac{\partial^2 T}{\partial x^2}+\frac{\partial^2 T}{\partial y^2}\right), \quad (4)$$

where u and v denote the respective velocities in the $x-$ and $y-$ directions respectively, ρ_f is the density of the base fluid, ν is the kinematic viscosity of the fluid, σ is the electrical conductivity, Λ_1 and Λ_2 are the relaxation and retardation times, α is the thermal diffusivity, T the fluid temperature, C the nanoparticle fraction,

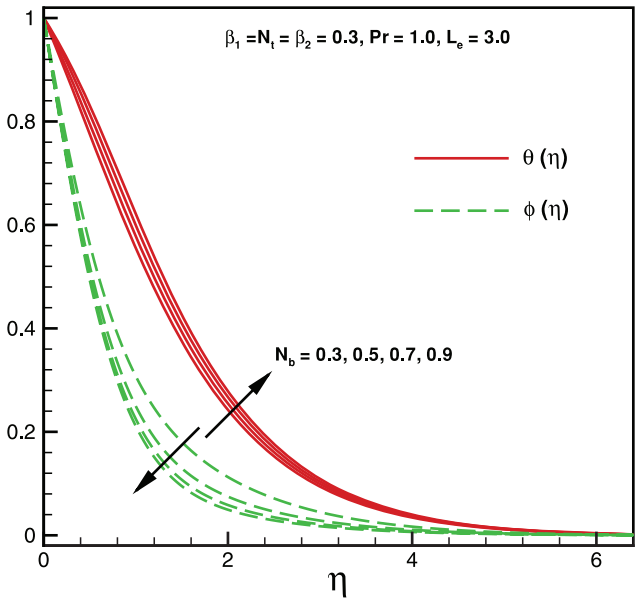

Figure 5. Variation of temperature and nanoparticles fraction for various values of N_b.
doi:10.1371/journal.pone.0069811.g005

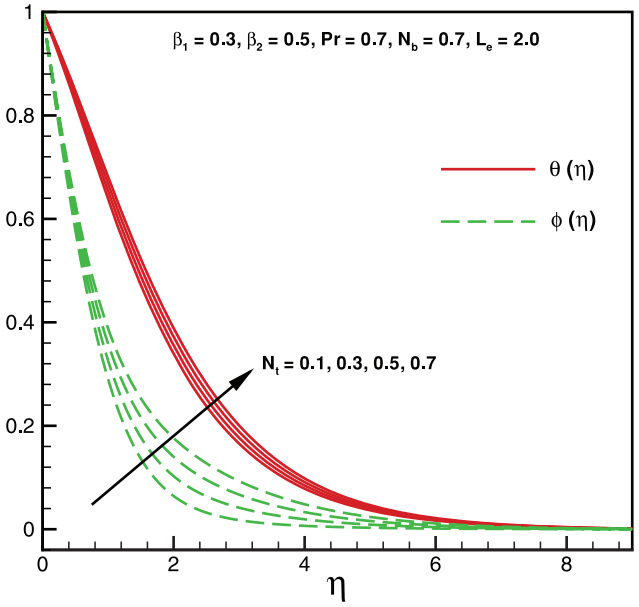

Figure 6. Variation of temperature and nanoparticles fraction for various values of N_t.
doi:10.1371/journal.pone.0069811.g006

T_w and C_w are the temperature of fluid and nanoparticle fraction at wall respectively, D_B the brownian diffusion coefficient, D_T is the thermophoretic diffusion coefficient, $\tau=\frac{(\rho c)_p}{(\rho c)_f}$ is the ratio between the effective heat capacity of the nanoparticle material and heat capacity of the fluid, C is the volumetric volume expansion coefficient and ρ_p is the density of the particles. When y tends to infinity then the ambient values of T and C are denoted by T_∞ and C_∞. The associated boundary conditions of Eqs. (2)–(4) are

$$\begin{aligned} &u=u_w(x)=ax,\ v=0,\ T=T_w,\ C=C_w \text{ at } y=0,\\ &u=0,\ v=0,\ T=T_\infty,\ C=C_\infty \text{ as } y\to\infty. \end{aligned} \quad (5)$$

Introducing the following similarity transformations

$$\psi=(a\nu)^{1/2}xf(\eta),\quad \theta(\eta)=\frac{T-T_\infty}{T_w-T_\infty},\quad \phi(\eta)=\frac{C-C_\infty}{C_w-C_\infty},\quad \eta=\sqrt{\frac{a}{\nu}}y, \quad (6)$$

where the stream function ψ is define as $u=\frac{\partial\psi}{\partial y}$ and $v=-\frac{\partial\psi}{\partial x}$. Making use of Eq. (6), Equation of continuity is identically satisfied and Eqs. (2) to (4) along with (5) take the following form

$$f'''-(f')^2+ff''+\beta_1\left(f^2f''''-2ff'f''\right)+\beta_2\left(ff''''-(f'')^2\right)=0, \quad (7)$$

$$\theta''+\Pr\left(f\theta'+N_b(\theta'\phi')+N_t(\theta')^2\right)=0, \quad (8)$$

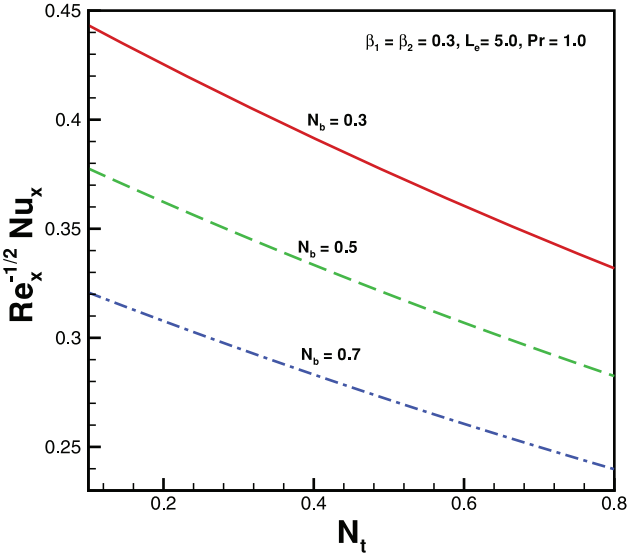

Figure 7. Variation of Nusselt number with N_t for various values of N_b when $\Pr < L_e$.
doi:10.1371/journal.pone.0069811.g007

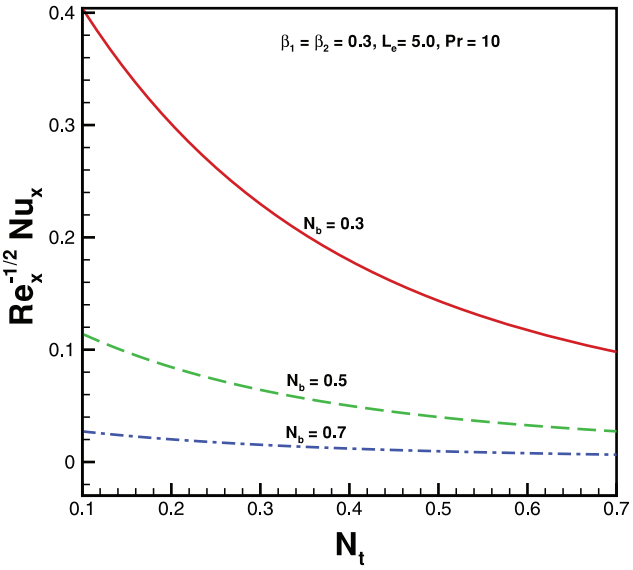

Figure 8. Variation of Nusselt number with N_t for various values of N_b when $\Pr > L_e$.
doi:10.1371/journal.pone.0069811.g008

$$\phi'' + L_e \Pr(f\phi') + \frac{N_t}{N_b}\theta'' = 0, \tag{9}$$

$$f(0) = 0, \quad f'(0) = 1, \quad f'(\infty) = 0, \quad f''(\infty) = 0, \tag{10}$$

$$\theta(0) = 1, \ \theta(\infty) = 0, \tag{11}$$

$$\phi(0) = 1, \ \phi(\infty) = 0, \tag{12}$$

in which prime indicates the differentiation with respect to η, $\beta_1 = a\Lambda_1$ and $\beta_2 = a\Lambda_2$ are the Deborah numbers in terms of relaxation and retardation times, respectively, $\Pr = \frac{\nu}{\alpha}$ is Prandtl number, $N_b = \frac{(\rho c)_P D_B(\phi_w - \phi_\infty)}{\nu(\rho c)_P}$ Brownian motion, $N_t = \frac{(\rho c)_P D_T(T_w - T_\infty)}{\nu(\rho c)_P}$ thermophoresis parameter, $L_e = \alpha/D_B$ the Lewis number. Expressions for the local Nusselt number Nu and the local Sherwood number Sh are

$$Nu_x = \frac{xq_w}{\alpha(T_w - T_\infty)}, \ Sh_x = \frac{xq_m}{D_B(C_w - C_\infty)}, \tag{13}$$

where q_w and q_m are the heat flux and mass flux, respectively.

$$q_w = -\alpha\left(\frac{\partial T}{\partial y}\right)_{y=0}, \ q_m = -D_B\left(\frac{\partial C}{\partial y}\right)_{y=0}. \tag{14}$$

Dimensionless form of Eq. (13) take the form

$$\mathrm{Re}_x^{-1/2} Nu_x = -\theta'(0), \quad \mathrm{Re}_x^{-1/2} Sh_x = -\phi'(0). \tag{15}$$

where $\mathrm{Re}_x = u_w(x)x/\nu$ is local Reynolds number based on the stretching velocity $u_w(x)$.

Results and Discussion

The nonlinear coupled ordinary differential equations (7)–(9) subject to the boundary conditions (10)–(12) have been solved numerically using the fourth-fifth order Runge-Kutta-Fehlberg method. Figs. 1, 2, 3, 4, 5, and 6 illustrate the behavior of emerging parameters such relaxation time constant β_1, retardation time constant β_2, Prandtl parameter Pr, Brownian parameter N_b, thermophoresis parameter N_t and Lewis number L_e on velocity profile $f'(\eta)$, temperature profile $\theta(\eta)$ and mass fraction function $\phi(\eta)$. Fig. 1, depicts the variation of β_1 on $f'(\eta)$, $\theta(\eta)$ and $\phi(\eta)$.

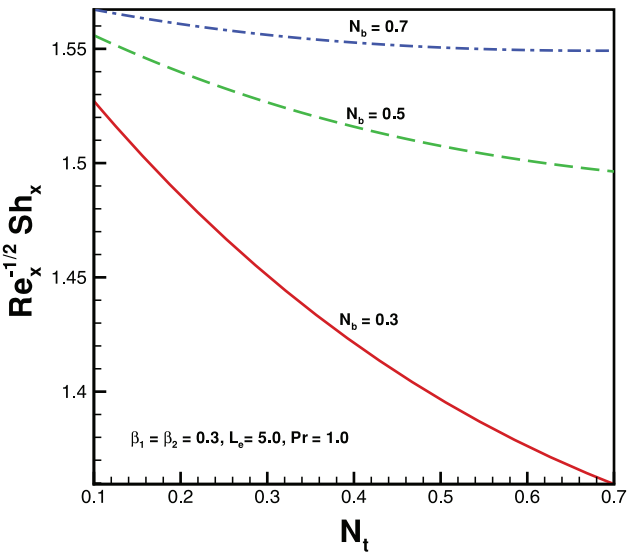

Figure 9. Variation of Sherwood number with N_t for various values of N_b when $\Pr < L_e$.
doi:10.1371/journal.pone.0069811.g009

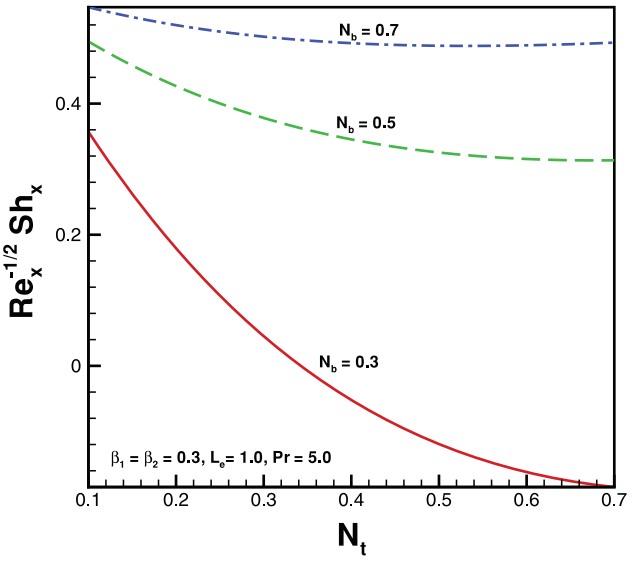

Figure 10. Variation of Sherwood number with N_t for various values of N_b when $\Pr > L_e$.
doi:10.1371/journal.pone.0069811.g010

Since β_1 is a function of relaxation time Λ_1 and due to viscoelastic properties of fluid it always resist the motion of the fluid. As a result, the velocity profile $f'(\eta)$ and boundary layer thickness are decreasing function of β_1. On the other hand, both temperature profile $\theta(\eta)$ and mass fraction function $\phi(\eta)$ increases with an increase in Deborah number β_1 (see Fig. 1). Physical behavior of Fig. 2 is due to an increase in retardation time of any material enhances the flow. Consequently, with an increase of β_2 velocity profile increases and both temperature and mass fraction function decreases (see Fig. 2). Thus, it concluded that β_1 and β_2 have opposite results on $f'(\eta)$, $\theta(\eta)$ and $\phi(\eta)$ due to relaxation and retardation times, respectively (see Fig. 1 and 2).

Physically it is observed that an increase in the elastic parameter, the resistance to fluid flow will increase. Table 1 illustrates an excellent agreement of the present results with Khan and Pop [17] in the absence of non-Newtonian parameters β_1 and β_2. As expected, it is found from Fig. 3, that both temperature and nanoparticle concentration profiles exert the decreasing behavior with the influence of Pr. Fig. 4 shows that both temperature and nanoparticle concentration have the same behavior when it is compared with Fig. 3 for higher values of L_e. Consequently,

Table 1. Comparison of Numerical Values for local Nusselt number $\mathrm{Re}_x^{-1/2}\,Nu_x$ and the local Sherwood number $\mathrm{Re}_x^{-1/2}\,Sh_x$ in the absence of non-Newtonian parameters when $\Pr = 10$ and $L_e = 1$.

N_t	Present results		Khan and Pop [17]	
	$-\theta'(0)$	$-\phi'(0)$	$-\theta'(0)$	$-\phi'(0)$
0.1	0.9524	2.1294	0.9524	2.1294
0.2	0.6932	2.2732	0.6932	2.2740
0.3	0.5201	2.5286	0.5201	2.5286
0.4	0.4026	2.7952	0.4026	2.7952
0.5	0.3211	3.0351	0.3211	3.0351

doi:10.1371/journal.pone.0069811.t001

Table 2. Comparison of Numerical Values for local Nusselt number $\mathrm{Re}_x^{-1/2}\,Nu_x$ in the absence of non-Newtonian parameters and nanoparticle.

$-\theta'(0)$		
Pr	**Present results**	**Wang [4]**
0.7	0.4582	0.4539
2.0	0.9114	0.9114
7.0	1.8954	1.8954
20	3.3539	3.3539
70	6.4622	6.4622

doi:10.1371/journal.pone.0069811.t002

boundary layer thickness decreases indefinitely with an increase in Pr. Effects of Brownian motion and thermophoresis parameters on temperature profile $\theta(\eta)$ and mass fraction function $\phi(\eta)$ are shown in Figs. 5 and 6. It is observed that for higher values of both N_b and N_t, the temperature profile rises. On the other hand Fig. 5, shows opposite behavior for mass fraction function when it is compare with Fig. 6, for increasing values of both N_b and Nt. In the absence of both nanoparticles and non-Newtonian effects there is an excellent agreement of the present results with Wang [4] (see Table 2). The effects of elastic parameter, Prandtl parameter, Brownian parameter, thermophoresis parameter and Lewis number on the Nusselt number and Sherwood number are presented in Figs. 7, 8, 9, and 10. It is seen from Fig. 7, 8 and Table 3 that the Nusselt number decreases with increasing N_t for both cases when Pr is less or greater than L_e for $N_b = 0.3, 0.5, 0.7$. Figs. 9 and 10 and Table 3 show the variation in dimensionless mass transfer rates vs N_t parameter for the selected values of other parameters. The dimensionless mass transfer rates decrease with the increase in N_t. Finally, high Prandtl fluid has a low thermal conductivity reducing conduction which results in an increase in the heat transfer rate at the surface of sheet.

Conclusions

In this study we have presented the Oldroyd-B fluid model for nanofluid over a stretching sheet. The effects of elastic parameter, Brownian motion and thermophoresis parameters on flow and heat transfer are discussed numerically. The main results of present analysis are listed below.

- Effects of β_1 and β_2 have opposite behavior for velocity, temperature and mass fraction function. These phenomena

Table 3. Numerical Values for local Nusselt number $\mathrm{Re}_x^{-1/2}\,Nu_x$ and the local Sherwood number $\mathrm{Re}_x^{-1/2}\,Sh_x$ in the presence of nanoparticle with $\beta_1 = \beta_2 = 0.3, L_e = 1$ and $\Pr = 6$.

N_t	$N_b = 0.3$		$N_b = 0.5$		$N_b = 0.7$	
	$-\theta'(0)$	$-\phi'(0)$	$-\theta'(0)$	$-\phi'(0)$	$-\theta'(0)$	$-\phi'(0)$
0.3	0.33988	1.83935	0.14820	1.87035	0.06012	1.84885
0.5	0.24099	1.95862	0.10486	1.94572	0.04255	1.90081
0.7	0.17918	2.06659	0.07792	2.00568	0.03163	1.94018

doi:10.1371/journal.pone.0069811.t003

only occur due to the effects of viscoelastic parameters β_1 and β_2.

- Both temperature and mass fraction function give same behavior for Pr and L_e. Since Pr is the ratio of kinematic to dynamic viscosity. Indeed for higher values of Pr, temperature profile remains under control.
- Effects of N_b and N_t for temperature profile are similar. Since both N_b and N_t causes to enhance the temperature.
- Effects of N_b and N_t for mass fraction function are opposite. Mathematically, it is seen that both N_b and N_t appeared in the function in Eqn. (9). Consequently, behavior of mass fraction function profile will be opposite for various values of both N_b and N_t.
- The magnitude of the local Nusselt numbers decreases for higher values of N_b.
- The magnitude of the local Sherwood numbers increases for higher values of N_b.

Author Contributions

Conceived and designed the experiments: RUH SN NSA CL ZHK. Performed the experiments: RUH SN NSA CL ZHK. Analyzed the data: RUH SN NSA CL ZHK. Contributed reagents/materials/analysis tools: RUH SN NSA CL. Wrote the paper: RUH SN NSA CL ZHK.

References

1. Sakiadis BC (1961) Boundary layer behavior on continuous solid flat surfaces. J AICHE 7: 26–28.
2. Tsou FK, Sparrow EM, Goldstein RJ (1967) Flow and heat transfer in the boundary layer on a continuous moving surface. Int. J Heat Mass Transfer 10: 219–235.
3. Crane L (1970) Flow past a stretching plate. Z ANGEW MATH PHYS 21: 645–647.
4. Wang CY (1989) Free convection on a vertical stretching surface. J App Math Mech (ZAMM) 69: 418–420.
5. Elbashbeshy EMA (2001) Heat transfer over an exponentially stretching continuous surface with suction. Arch Mech 53: 643–651.
6. Khan SK, Abel MS, Sonth RM (2004) Visco-elastic MHD Flow Heat and Mass Transfer Over a Stretching Sheet with Dissipation of Energy and Stress Work. Heat Mass Transfer 40: 7–57.
7. Ishak A, Nazar R, Pop I (2008) Heat transfer over a stretching surface with variable heat flux in micropolar fluids. Phys Lett A 372: 559–561.
8. Nadeem S, Zaheer S, Fang T (2011) Effects of thermal radiation on the boundary layer flow of a Jeffrey fluid over an exponentially stretching surface. Numer Algorithms 57: 187–205.
9. Nadeem S, Haq R, Lee C (2012) MHD flow of a Casson fluid over an exponentially shrinking sheet. Scientia Iranica B19: 1550–1553.
10. Choi SUS (1995) Enhancing thermal conductivity of fluids with nanoparticles. Development and applications of non-Newtonian flows. Siginer D.A. and Wang HP, eds, ASME MD- 231: 99–10.
11. Xuan Y, Roetzel W (2000) Conceptions for heat transfer correlation of nanofluids. Int J Heat Mass Trans 43: 3701–3707.
12. Khanafer K, Vafai K, Lightstone M (2003) Buoyancy-driven heat transfer enhancement in a two-dimensional enclosure utilizing nanofluids. Int J Heat Mass Tran 46: 3639–3653.
13. Nield DA, Kuznetsov AV (2009) The Cheng–Minkowycz problem for natural convective boundary-layer flow in a porous medium saturated by a nanofluid. Int J Heat Mass Trans 52: 5792–5795.
14. Kuznetsov AV, Nield DA (2010) Natural convective boundary- layer flow of a nanofluid past a vertical plate. Int J Therm Sci 49:243–247.
15. Hamad MAA, Ferdows M (2012) Similarity solutions to viscous flow and heat transfer of nanofluid over nonlinearly stretching sheet. Appl Math Mech Engl Ed 33: 923–930.
16. Hamad MAA, Ferdows M (2012) Similarity solution of boundary layer stagnation-point flow towards a heated porous stretching sheet saturated with a nanofluid with heat absorption/generation and suction/blowing: A lie group analysis. Commun Nonlinear Sci Numer Simulat 17: 132–140.
17. Khan WA, Pop I (2010) Boundary-layer flow of a nanofluid past a stretching sheet. Int J Heat Mass Trans 53: 2477–2483.
18. Akbar NS, Nadeem S, Hayat T, Hendi AA (2012) Peristaltic flow of a nanofluid in a non-uniform tube. Heat Mass Transfer 48: 451–459.
19. Akbar NS, Nadeem S, Hayat T, Hendi AA (2012) Peristaltic flow of a nanofluid with slip effects. Meccanica 47: 1283–1294.
20. Akbar NS, Nadeem S (2012) Peristaltic flow of a Phan-Thien-Tanner nanofluid in a diverging tube. Heat transfer Asian Research 41: 10–22.
21. Ellahi R, Hayat T, Mahomed FM, Zeeshan A (2010) Exact solutions of flows of an Oldroyd 8-constant fluid with nonlinear slip conditions. Z Fur Naturforsch A 65: 1081–1086.
22. Khan M, Ellahi R (2009) Exact solution for oscillatory rotating flows of a generalized Oldroyd-B fluid through porous medium. J Porous Media1 2: 777–788.
23. Ellahi R, Raza M, Vafai K (2012) Series solutions of non-Newtonian nanofluids with Reynolds' model and Vogel's model by means of the homotopy analysis method. Math Comp Model 55: 1876–1891.
24. Zeeshan A, Ellahi A, Siddiqui AM, Rahman HU (2012) An investigation of porosity and magnetohydrodynamic flow of non- Newtonian nanofluid in coaxial cylinders. Int J Phys Sci 7: 1352–1361.
25. Makinde OD, Khan WA, Khan ZH (2013) Buoyancy effects on MHD stagnation point flow and heat transfer of a nanofluid past a convectively heated stretching/shrinking sheet. Int J Heat Mass Trans 62: 526–533.